Potent and Selective Inhibition of Membrane-Type Serine Protease 1 by Human Single-Chain Antibodies[†]

Jeonghoon Sun, Jaume Pons,[‡] and Charles S. Craik*

*Department of Pharmaceutical Chemistry, University of California, San Francisco, 513 Parnassus,
San Francisco, California 94143*

ABSTRACT: Specific human antibodies targeting proteases expressed on cancer cells can be valuable reagents for diagnosis, prognosis, and therapy of cancer. To this end, a phage-displayed antibody library was screened against a cancer-associated serine protease, MT-SP1. A protein inhibitor of serine proteases that binds to a defined surface of MT-SP1 was used in an affinity-based washing procedure. Six antibodies were selected on the basis of their ELISA profiles and ability to serve as useful immunological reagents. The apparent K_i, indicative of the potency of the antibodies at inhibiting human MT-SP1 activity, ranged from 50 pM to 129 nM. Two of the antibodies had approximately 800-fold and 1500-fold selectivity when tested against the most homologous serine protease family member, mouse MT-SP1, that exhibits 86.6% sequence identity. Surface plasmon resonance was used as an independent means of determining the binding constants of the six antibodies. Association rates were as high as 1.15×10^7 s^{-1} M^{-1}, and dissociation rates were as low as 3.8×10^{-4} s^{-1}. One antibody was shown to detect denatured MT-SP1 with no cross reactivity to other family members in HeLa or PC3 cells. Another antibody recognized the enzyme in human prostate tissue samples for immunohistochemistry analysis. The mode of binding among the six antibodies and the protease was analyzed by competition ELISA using three distinctly different inhibitors that mapped the enzyme surface. These antibodies constitute a new class of highly selective protease inhibitors that can be used to dissect the biological roles of proteolytic enzymes as well as to develop diagnostic and therapeutic reagents.

Proteases are involved in all stages of cancer progression including growth, angiogenesis, invasion, migration, and metastasis (*1*−*6*). At the crux of cancer pathogenesis is metastasis during which unregulated proteases lead to invasive remodeling of the extracellular matrix (*7*−*10*). Therefore, inhibitors targeting these proteases have been developed. Although partially effective as tools to study cancer progression and metastasis, small-molecule inhibitors are plagued by problems with resistance and toxicity, while macromolecular inhibitors can suffer from promiscuity and low activity. Moreover, proteases are widely distributed in nature comprising approximately 2% of the entire human genome (*11*). This omnipresence of proteases with nearly identical active site elements creates the need to develop a general method for producing potent, highly selective inhibitors.

Validating a protease as an appropriate therapeutic target for cancer is a challenging task. The recent discovery of the type II transmembrane serine proteases that have been detected at high levels in various cancer cell lines has underscored their potential role in cancer (*4*, *5*, *8*). One member of this family, membrane-type serine protease 1 (MT-SP1),[1] has been implicated as a key protease in triggering the plasminogen proteolytic cascade, a central pathway in cancer progression and metastasis. MT-SP1 is expressed in human tissues such as prostate, breast, and ovary (*12*−*15*). MT-SP1 is a mosaic protein of 855 amino acids and is composed of a short cytosolic N-terminal region, a transmembrane signal anchor, several protein−protein interaction domains, and a C-terminal protease domain. The serine protease domain at the C-terminus (hMT-SP1-P) is strategically positioned on the cell surface to allow for efficient interaction with other proteins, thus making it a potentially recognizable epitope and a direct target for regulation of the protease activity (*12*).

Since MT-SP1 is expressed on the cell surface, where large molecules can easily access the protease domain, human monoclonal antibodies (MAbs) were explored for their application in inhibitor design. As therapeutic reagents, human MAbs can be far less toxic and more selective inhibitors than both small molecule and other macromolecular inhibitors. Furthermore, MAbs can easily be developed

* To whom correspondence should be addressed. Mailing address: 513 Parnassus Box 0446, University of California, San Francisco, San Francisco, CA 94143-0446. Telephone number: 415-476-8146. Fax: 415-502-8298. E-mail address: craik@cgl.ucsf.edu.

‡ Current address: Rinat Neuroscience corporation, 3155 Porter Drive, Palo Alto, CA 94304.

1 Abbreviations: ¹MT-SP1, membrane-type serine protease 1; scFv, single chain variable fragment; ELISA, enzyme-linked immunosorbent assay; hMT-SP1-P, protease domain of human MT-SP1; YT, yeast extract:tryptone.

as general tools to further investigate unidentified roles of MT-SP1 (*16*). MAbs are heterodimeric proteins, and the light- and heavy-chain variable domains can be linked together by a peptide spacer and expressed as one chain. This chimeric protein is referred to as a single chain Fv (scFv) (*17, 18*). In comparison to full-length antibodies, the scFv is a small monomeric single chain that is more amenable to manipulation by genetic recombination, large-scale bacterial protein expression, and phage display. Yet scFvs retain antibody-like specificity and affinity, and the scFv scaffold can be expanded to the Fab or the full IgG as needed.

Avoiding the restraints of conventional hybridoma approaches, phage display is an efficient method that can be inventively applied for direct selection of human scFvs (*19, 20*). As the quality of the primary library is certainly one of the most important components, we chose a phage-displayed human combinatorial scFv library (*21*). This library was synthetically constructed mimicking the human antibody repertoire in terms of structure, amino acid sequence diversity, and germline usage with seven V_H and seven V_L families covering greater than 95% of the human antibody diversity (*22−24*). Containing approximately 2×10^9 members, this library provides large diversity with low redundancy (*21*).

We report here in vitro selection of human scFv inhibitors of the catalytic domain of MT-SP1 via phage display aided by an affinity washing procedure. Enzyme inhibition assays, kinetic analysis of binding, immunoblotting, and immunohistochemical staining were performed for characterization of these scFvs. Well-characterized small molecule and macromolecular serine protease inhibitors were used in a competition ELISA to probe the binding interactions of the scFvs to the protease. Highly potent, inhibitory scFvs of various binding modes and selectivity were developed for human MT-SP1 to assist in evaluating its physiological role.

EXPERIMENTAL PROCEDURES

Media and Buffers. The components of reaction media and buffers used are listed below. *BBS*: 200 mM boric acid, 150 mM NaCl, 2 mM EDTA, 20% sucrose, pH 8.0. *HBS-EP*: 10 mM HEPES, 150 mM NaCl, 3 mM EDTA, 0.05% polysorbate 20 (Tween 20), pH 7.4. *LB*: 1% tryptone, 0.5% yeast extract, 1% NaCl, pH 7.0. *LB-1*: LB, 34 μg mL^{-1} chloramphenicol, 1% glucose. *NP-40 lysis buffer*: 50 mM Tris·HCl, 150 mM NaCl, 1.0% NP-40. *PBS*: 0.9% NaCl, 10 mM sodium phosphate, pH 7.2. *MPBS*: PBS, 5% nonfat milk, pH 8.0. *PBST*: PBS, 0.05% Tween 20. *PPB*: 30 mM Tris·HCl, 1 mM EDTA, 20% sucrose, pH 8.0. *TBS*: 150 mM NaCl, 10 mM Tris·HCl, pH 7.5. *TBST*: TBS, 0.05% Tween 20; *MTBST*: TBST, 5% nonfat milk. *TBSTCa*: TBST, 1 mM CaCl$_2$. *YT*: 0.5% tryptone, 0.5% yeast extract, 0.5% NaCl. *YT-1*: 2 × YT, 34 μg mL^{-1} chloramphenicol, 0.1 mM isopropyl D-thiogalactoside (IPTG). *YT-2*: 2 × YT, 34 μg mL^{-1} chloramphenicol, 1% glucose. *YT-3*: 2 × YT, 34 μg ml^{-1} chloramphenicol, 0.1% glucose, 1 mM IPTG; *YT-4*: 2 × YT, 34 μg mL^{-1} chloramphenicol.

Affinity Selection. All experiments were performed at room temperature unless specifically mentioned. For round 1, 2 × 3 wells on a Maxisorp plate (Nalgenunc, Rochester, NY) and one well for control in another Maxisorp plate were coated with 10 μg of recombinant hMT-SP1-P (*12*) per well

in 300 μL of 50 mM NaHCO$_3$ buffer (pH 9.6), incubated 16 h at 4 °C, and washed with PBS. In the control well, 100 μL of Spectrozyme tPA (100 μM in 50 mM NaCl, 50 mM Tris·HCl (pH 8.8), and 0.01% Tween 20) was added to test the enzyme activity. The other antigen-coated wells were treated with a blocking buffer, MPBS, for 2 h with gentle shaking. The blocking solution was removed and rinsed twice with PBS. Meanwhile, 450 μL of the scFv phage library (*21*) was mixed with 450 μL MPBS containing 0.1% Tween 20. The preblocked phage mix was transferred into each well and incubated for 1 h. After the phage solution was removed, three of the wells for standard wash were rinsed five times with PBST and five times with PBS. The other three wells for the ecotin wash were rinsed with 100 nM ecotin-containing PBST five times and PBS five times. The ecotin variant used for this affinity wash was an engineered dimer that contains the sequence TSSRRA at positions 81−86 and an arginine at position 70. This mutant ecotin inhibits MT-SP1 at 50 pM using 100 μM of the substrate Spectrozyme tPA (American Diagnostica, Greenwich, Connecticut). *E. coli* TG1 cells were added, and the mixture was incubated for 45 min at 37 °C with gentle shaking. VCSM13 helper phage was added to each well and the mixture was incubated for 2 h at 37 °C. Aliquots from each well were set aside for titration and the rest was incubated for 16 h.

For round 2, 2 wells on a Maxisorp plate were coated with hMT-SP1-P and rinsed as in round 1 and blocked with 5% MPBS for 2 h. The TG1 cells were spun for 10 min at 2200g at 4 °C. Supernatants from the three wells of the standard wash were combined, as were the supernatants from the three wells of the ecotin wash. Each 165 μL of supernatant from the ecotin pool and the standard pool was added separately into each 165 μL of MPBS with 0.1% Tween 20. The two mixtures were incubated for 2 h with gentle shaking. Aliquots from each well were set aside for round 2 input titer. The blocking solution from the Maxisorp plate was removed, and each pre-blocked phage mix (300 μL) was transferred into each coated well and incubated for 1 h. After the phage solution was removed, one well (standard pool) was rinsed five times with PBST, incubated with PBST (5 × 5 min), and rinsed five times with PBS. The other well (ecotin pool) was rinsed five times with PBST, incubated with 100 nM ecotin in PBST (3 × 5 min), and rinsed five times with PBS. VCSM13 helper phage were added to each well, and the infected cells were transferred into shake flasks with 50 mL YT-1 and incubated for 16 h at 37 °C with gentle shaking. The overnight culture (1 mL) from the round 2 panning was stored in 15% glycerol at −80 °C as a polyclonal selection pool. The remaining 49 mL was spun, the cells were harvested, and the plasmid DNA was purified. A 864 bp *Xba* I/*EcoR* I fragment was purified and ligated into pMx7FH vector (*25*). The ligation mixture was electroporated into JM83 cells, and the cells were spread onto an LB-1 agarose plate that was incubated 16 h at 37 °C. Colonies were chosen, grown, and preserved in 15% glycerol at −80 °C.

Microexpression of ScFv. YT-2 was inoculated with scFv glycerol stock and incubated at 37 °C for 3 h with shaking at 250 rpm. Expression was induced at an A$_{600}$ of 0.5 by adding 100 μL YT-3, and the mixture was incubated for 4 h at 30 °C with gentle shaking. Cells were spun down, resuspended in 125 μL of ice-cold BBS, incubated at 4 °C
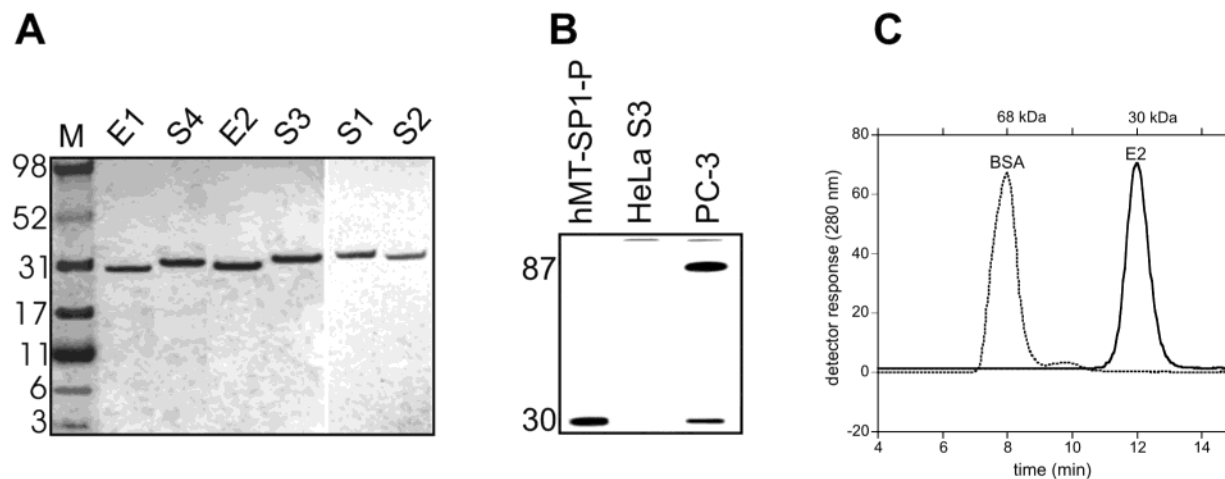
FIGURE 1: SDS−PAGE and western analyses. (A) SDS−PAGE analysis of the six scFvs after IMHC. This experiment was performed in reducing conditions. The molecular weight markers are shown in kilodaltons in the lane M. Other lanes show the scFvs that were used for further analyses. These scFvs produce a pure single band around 30 kDa. (B) Immunoblot analysis. S2 was used as the primary antibody. The recombinant hMT-SP1-P is shown at 30 kDa. HeLa S3 cells did not expressed MT-SP1. PC-3 cells produced full-length MT-SP1 at 87 kDa, along with the cleaved protease domain at 30 kDa. (C) Elution profiles of BSA (68 kDa) and E2 (30 kDa). BSA and E2 were run separately but represented in the same graph. Other scFvs, including E1, S1, S3, and S4, also eluted after approximately 12 min and only one major peak was observed as for E2.

for 16 h with shaking, and spun down. The supernatant was then transferred to a new 96 well plate.

ELISA. A Maxisorp plate was coated with 0.5 μg of hMT-SP1-P per well in 100 μL of 50 mM NaHCO$_3$ buffer (pH 9.6) and incubated overnight at 4 °C. The antigen in solution was removed, and the plate was rinsed with TBST and blocked for 1 h with MPBS. The scFv microexpressed supernatants (50 μL) (or various concentrations of isolated scFvs (50 μL)) and MPBS (50 μL) were added to each well and incubated for 1.5 h. Wells were then washed 5 times with TBST. Anti-Flag M2-HRP conjugate (100 μL, 1:15000 in TBST, Sigma, St. Louis, MO) was added to each well and incubated for 1 h. After 5 washes with TBST, peroxidase substrate BM blue POD substrate (Roche Diagnostics, Indianapolis, IN) was added, and the reactions were developed for 10 min and then stopped with the addition of 1 M H$_2$SO$_4$ (100 μL). The absorbance was determined at 450 nm using a microplate reader.

ScFv Expression and Protein Purification. A single bacterial colony containing the pMx7FH plasmids of each scFv was inoculated into YT-4 (10 mL), and the cells were grown overnight. One liter of YT-4 was inoculated with the scFv culture (2 mL) and incubated at 30 °C, 250 rpm. Expression was induced at an A_{600} of 0.5 by addition of IPTG to a final concentration of 0.5 mM. Incubation was continued for 16 h with vigorous shaking. Cells were harvested, resuspended in precooled PPB, and incubated for 30 min at 4 °C. Cells were collected and resuspended in precooled BBS and incubated overnight at 4 °C. The PPB and BBS supernatants were combined and spun to pellet more bacterial debris. The supernatant was filtered through a 0.2 μm filter. PCR was performed on the bacterial pellet for DNA sequencing. The His-tagged scFv fragments were purified by immobilized-metal ion affinity chromatography (IMAC) using Ni−NTA Agarose (Qiagen, Valencia, CA) according to the manufacturer's protocol and analyzed by SDS−PAGE and size exclusion chromatography (Figure 1c) using Superdex75 FPLC column (Amersham Pharmacia Biotech, Peapack, NJ). Each scFv was eluted in the MT-SP1 enzyme

assay buffer containing 50 mM NaCl, 50 mM Tris·HCl (pH 8.8), and 0.01% Tween 20.

Immunoblot Analysis. Samples including pure recombinant hMT-SP1-P and lysates of the HeLa S3 and PC-3 (*26*) cells were analyzed using a standard immunoblot protocol as previously reported (*13*) using the screened scFvs as primary antibodies and the anti-flag M2-HRP conjugate as a secondary antibody. The samples were boiled for 2−5 min at 100 °C in the presence of SDS and 2-mercaptoethanol. Electrophoresis was performed under a reducing conditions using SDS and 2-mercaptoethanol. The substrate for HRP was ECL (Amersham Pharmacia Biotech, Peapack, NJ).

Inhibition Assay. The initial reaction velocities of human MT-SP1, mouse MT-SP1, and trypsin were measured in 50 mM NaCl, 50 mM Tris·HCl (pH 8.8), and 0.01% Tween 20 with 100 μM Spectrozyme tPA (methyl-sulfonyl-D-cyclohexyltyrosyl-glycyl-L-arginine-p-nitroanilide) as a substrate and various concentrations of scFvs. Inhibition constants were evaluated by fitting to the equation for tight-binding inhibitors (*27*).

Binding Kinetics. The association and dissociation rate constants were obtained by surface plasmon resonance using a BIAcore Biosensor 2000 (Upsala, Sweden). The hMT-SP1-P (ligand), in 10 mM glycine·HCl, pH 3.0, was covalently immobilized onto a CM5 chip according to the manufacturer's protocol. The hMT-SP1-P was stable for 7 days at pH 3.0, and its proteolytic activity was recovered in HBS-EP running buffer. Low-density surfaces (<100 RU) and high flow rates (50 μL min^{-1}) were used for kinetic parameter determinations. The scFvs (analytes) were dialyzed in running buffer HBS-EP to minimize bulk refractive index differences. Surface regenerations were performed with a 25 μL pulse of ImmunoPure Gentle Ag/Ab elution Buffer (Pierce, Rockford, IL). The reference channel was treated using the same chemistry as the ligand coupled surface. The sensorgram of the reference surface was subtracted from the ligand conjugated surface for each injection, and multiple injections of running buffer were averaged and subtracted from the whole data set to remove mechanical noise. A series

Table 1: Amino Acid Sequences of the CDR3[a]

ScFv	V$_L$ template	V$_L$ sequence	V$_H$ template	V$_H$ sequence
E1	Vκ1	QYSNFPSTF	VH3	LPYYGRPGGYRFFDV
E2	Vκ1	QHGNLPYTF	VH3	PYLTYPQRRGPQNVSPFDN
S1	Vλ1	SYDGNSQNF	VH3	RGGYGVWSGWHGYHFDY
S2	Vκ2	QMSNFPMTF	VH3	HKTNSFRHLRATFPDFDV
S3	Vλ2	LSYDRFLT	VH1A	QHRGHTYGRGYKIFFDP
S4	Vλ1	SRDISQY	VH1A	FHIRRYRSGYYDKMDH

[a] The CDR3 region of V$_L$ were randomized with 4−21 residue variations and the CDR3 of V$_H$ with 7−30 residues. All combinations of other variable regions were fixed in 49 templates from the master repertoires comprising 7 light chains and 7 heavy chains (*21*).

of analyte concentrations ranging from 100 to 0.1 nM were injected, and data were fit globally to obtain association and dissociation kinetic parameters using a 1:1 Langmuir binding model in the BIAevaluation 3.1 software. All kinetic rates reported are the average of two independent determinations on three different surfaces. The data for the low affinity binder S2 were estimated by steady-state affinity fitting using the same software. No mass transfer problems were detected by injecting analytes at 5, 15, and 75 μL min^{-1} on low-density surfaces. Different injection times (0.5, 5, 20 min) of 100 nM analyte did not show any evidence of linked reactions.

Competition ELISA. A competition ELISA in the presence of ecotin (10 nM), mono ecotin (400 nM), H-D-Phe-Pro-Arg-chloromethyl ketone (CMK: Bachem, Torrence, CA) (100 nM), or benzamidine (10 mM) was performed by standard ELISA methods, except that ecotin, mono ecotin, CMK, or benzamidine were added to each well and incubated 1 h before scFv was added.

Immunohistochemistry (IHC). IHC studies were performed on paraffin-embedded or frozen samples from prostate tissues. Sections were cut at 5 μm and placed on pretreated slides (Fisher Scientific, Yorba Linda, CA). In the case of the paraffin-embedded sections, the antigen was retrieved and fixed using Citra (Biogenx, San Ramon, CA) according to the manufacturer's protocol. The frozen sections were fixed using a standard acetone fix method. Prior to immunostaining, sections were treated by peroxide block, avidin−biotin block, and protein block sequentially. Sections were incubated with each scFv and link at various concentrations. Peroxide-conjugated streptavidin label was applied. The antigen−antibody complex was localized by the chromogen 3-amino-9-ethylcarbazole. Sections were counterstained with aqueous hematoxylin before gelatin-mounting medium was applied.

RESULTS

Phage Selection. Round 1 panning began with screening the scFv phage library (*21*) against immobilized, active hMT-SP1-P. Selection with two separate pools of washing solutions, namely, "standard" and "ecotin" pools, were carried out. The wash solution for the standard pool was TBS containing Tween 20. In the ecotin pool, ecotin, a macromolecular inhibitor specific for trypsin-fold serine proteases (*28−31*), was added to TBS containing Tween 20 as a competitive component to isolate more potent protease inhibitors. After washing, the surviving phage-displayed scFvs were incubated with *E. coli* cells and inoculated with helper phage, to generate a new repertoire for round 2. The numbers of surviving titers were 10^5 in the ecotin pool and

1.5 × 10^5 in the standard pool out of the initial 3 × 10^{10} phage-displayed scFvs in each pool.

In round 2 panning, more elongated washing times were applied for both standard and ecotin pools. The numbers of titers of both pools drastically decreased; out of 1.5 × 10^{10} provided, only 90 survived in the ecotin pool and 165 in the standard pool. The surviving phage were incubated with *E. coli* cells, and those cells were grown and harvested. Plasmid DNA were isolated, digested with restriction endonucleases, and subcloned into a vector for scFv expression that includes a hexahistidine tag at the C-terminus. The expression vector harboring selected scFv genes were electroporated into *E. coli* cells that were subsequently plated onto LB agarose plates. For each pool, 96 colonies were picked, grown, and lysed.

ELISA was performed using the cell lysates containing scFv to estimate binding affinity of scFv to the target antigen hMT-SP1-P. From the standard pool, 24 scFvs were ELISA-positive, while only 7 scFvs were ELISA-positive in the ecotin pool. The variants that emitted the strongest ELISA signals, four scFvs from the standard pool and two from the ecotin pool, were chosen for further characterization. Because the ELISA signal is undetectable for scFvs expressed at extremely low levels, our system was capable at selecting the scFv variants possessing high binding affinity to hMT-SP1-P as well as reasonable protein expression levels.

Isolation of the ScFvs and Sequence Analysis. The variants that were characterized further were E1 and E2 from the ecotin pool and S1, S2, S3, and S4 from the standard pool. The letter "E" denotes the variant from the ecotin pool and "S" the variant from the standard pool. The sequences of the V$_L$ and V$_H$ regions that were determined by DNA sequencing are shown in Table 1. The six clones yielded six independent, unique sequences.

The library was originally constructed using 49 templates by shuffling 7 heavy-chain templates and 7 light-chain templates (*21*). As shown in Table 1, primarily VH3 templates were chosen for the heavy chain while a variety of templates were chosen for the light chain. The complementarity determining region (CDR) 3 of the heavy and light chains were designed to vary in the composition and size of the sequence. The number of amino acids in heavy chain CDR3 ranges from 15 to 19 residues and the light chain CDR3 ranges from 7 to 9. The CDR3 of the V$_H$ was randomized with 5−28 residues, and the CDR3 of the V$_L$ was randomized with 4−21 residues (*21*).

Inhibition Analysis. The purified scFvs were analyzed by SDS−PAGE and Coomassie Brilliant blue staining (Figure 1a), and size-exclusion chromatography (Figure 1c) to validate that the scFvs were pure monomeric proteins. To

Table 2: Inhibition Analysis

ScFv	K_i^* (nM)[a] (hMT-SP1)[b]	K_i^* (nM) (mMT-SP1)[c]	K_i^*(mMT-SP1) K_i^*(hMT-SP1)
E1	2 ± 0.14	>200	>100
E2	0.05 ± 0.01	40 ± 10	800
S1	129 ± 3	NI[d]	—
S2	> 500	NI	—
S3	40 ± 4	NI	—
S4	0.59 ± 0.02	>900	1525

[a] Inhibition analysis was performed at 25 °C. The protease concentration was 1 nM for all scFvs except E2. For E2 40 pM hMT-SP1 and 1 nM mMT-SP1 were used. The initial reaction velocities of human MT-SP1, mouse MT-SP1, and rat trypsin were measured in 50 mM NaCl, 50 mM Tris·HCl (pH 8.8), 0.01% Tween 20, 100 μM Spectrozyme tPA (methyl-sulfonyl-D-cyclohexyltyrosyl-glycyl-L-arginine-p-nitroanilide), and various concentrations of the scFvs. The K_m of Spectrozyme tPA for hMT-SP1 is 31.4 ± 4.2 μM (12). K_i^*s were evaluated by fitting to the equation for tight-binding inhibitors (27). $K_i^* = K_i (1 + [S]/K_m)$, [S] = substrate concentration. All of these scFvs did not inhibit rat trypsin to any appreciable extent. [b] Recombinant protease domain of human MT-SP1 (hMT-SP1-P) was tested. [c] Recombinant protease domain of mouse MT-SP1 (epithin-P) was tested. [d] NI stands for "no inhibition".

Table 3: Kinetics of Binding between Human MT-SP1 and ScFvs

ScFv	k_{on} (10^6 s^{-1} M^{-1})[a]	k_{off} (10^{-3} s^{-1})[a]	K_d (nM)[b]
E1	0.63 ± 0.02	1.1 ± 0.2	1.8 ± 0.3
E2	2.1 ± 0.5	0.38 ± 0.07	0.16 ± 0.01
S1	1.5 ± 0.3	1.9 ± 0.1	1.3 ± 0.4
S2	—	—	>500[c]
S3	1.7 ± 0.2	2.5 ± 0.5	1.5 ± 0.2
S4	11.5 ± 2	5.8 ± 0.4	0.51 ± 0.06

[a] From global fitting of the sensorgram data to a 1:1 Langmuir binding model in BIAevaluation 3.1 software. [b] Average and standard deviation of k_{off}/k_{on} for each repeat. [c] Estimated by steady-state affinity.

Table 4: Competition ELISA[a]

scFv	no ecotin	ecotin	mono ecotin	CMK	benzamidine
E1	+	−	−	−	+
E2	+	−	−	−	−
S1	+	−	−	−	−
S2	+	+	+	+	+
S3	+	−	−	−	−
S4	+	−	−	−	−

[a] ELISA was performed with hMT-SP1-P only and in the presence of ecotin (10 nM), mono ecotin (400 nM), H-D-Phe-Pro-Arg-chloromethyl ketone (CMK) (100 nM), or benzamidine (10 mM) with various concentrations of scFvs. Concentrations of the competitors were chosen at least 10 times higher than their K_i values against hMT-SP1.

determine the potency and specificity of the scFv to MT-SP1, inhibition assays were performed with the human MT-SP1 protease domain (hMT-SP1-P), mouse MT-SP1 protease domain (epithin-P), and rat trypsin. The initial reaction velocities were measured for several concentrations of the scFvs using Spectrozyme tPA as a substrate. Apparent inhibition constants were evaluated by fitting to a model of tight-binding inhibitors (27). The results are indicated in Table 2. The sequences of hMT-SP1-P and epithin-P exhibit 86.6% identity of amino acids. Since epithin-P shares such a high sequence identity with hMT-SP1-P, the difference in inhibition between these enzymes is a reasonable indicator of the selectivity of these scFvs. Rat trypsin has 35% amino acid sequence identity with MT-SP1 and was chosen as a control for general serine protease inhibition by the scFvs. We used the ratio of the apparent inhibition dissociation constant (K_i^*) of hMT-SP1-P and epithin-P as a selectivity parameter.

All of the six scFvs inhibited hMT-SP1-P at far lower concentrations than epithin-P and did not inhibit rat trypsin to any appreciable extent. The selectivity for hMT-SP1-P over epithin-P was more than 100-fold with E1, 800-fold with E2 and 1500-fold with S4. Among these scFvs, E2 was the most potent inhibitor with a K_i^* of 50 pM for hMT-SP1-P and 40 nM for epithin-P. S4 was the most selective, inhibiting hMT-SP1-P with a K_i^* of 0.59 nM and epithin-P at greater than 900 nM. S1 and S3 moderately inhibit hMT-SP1-P but do not inhibit epithin-P measurably.

Binding Kinetics. The binding kinetics of the six scFvs to hMT-SP1-P was further characterized by surface plasmon resonance (Figure 2). The association (k_{on}) and dissociation (k_{off}) rates were measured, and the dissociation equilibrium constant (K_d) was calculated (Table 3). For E1, E2 ,and S4, the K_d correlates well with the K_i^* values, while the K_i^* values of S1 and S3 were 27−100-fold higher than their K_d values. S4 exhibited an unusually fast association rate (1.2×10^7 s^{-1} M^{-1}), while E2 and E1 dissociate slower than other scFvs.

Mode of Binding. With the isolated scFvs, competition ELISA was performed in the presence of ecotin variants or smaller protease inhibitors, including a peptidyl chloromethyl ketone (CMK), and benzamidine (Table 4, Figure 3). Mono ecotin (30) is an engineered ecotin variant that was designed to be monomeric and binds only to the active site of trypsin-fold serine proteases inhibiting the enzyme activity of MT-SP1 at 75 nM K_i^*. In the presence of ecotin, mono ecotin, or CMK, only S2 was ELISA-positive, indicating that S2 binds a site where these inhibitors do not bind and the rest of the scFvs bind at or close to the active site. With benzamidine, which blocks the S1 pocket of MT-SP1, E1 and S2 were ELISA-positive, suggesting that these scFvs do not involve interactions with the S1 pocket.

Immunoblotting. Immunoblot analysis of the 6 scFvs were performed with hMT-SP1-P, and a prostate cancer cell line (PC-3) (26) that expresses the full-length MT-SP1. HeLaS3 cells were used as a control cell line that does not express MT-SP1. Among the scFvs, only S2 recognized the denatured antigen, as represented in Figure 1b.

Immunohistochemistry (IHC). The IHC examinations of a fraction of whole tumor tissues from randomly chosen cancer patients revealed that only S1 of the six scFvs tested stained MT-SP1 expressed in the tissues (Figure 4). It was indicated that MT-SP1 is localized in the lumenal membrane in both the normal prostate tissue and tumor prostate tissue (Figure 4). Noteworthy is the shedding of MT-SP1 into the lumen (Figure 4b) in a metastatic prostate cancer tissue sample, suggesting MT-SP1 is shed from the surface of the epithelial cell.

DISCUSSION

Technical advances in protein engineering have extended the original roles of antibodies in the molecular defense system by creating novel functions on the antibody scaffold (32−36). Since antibodies feature high-affinity binding with
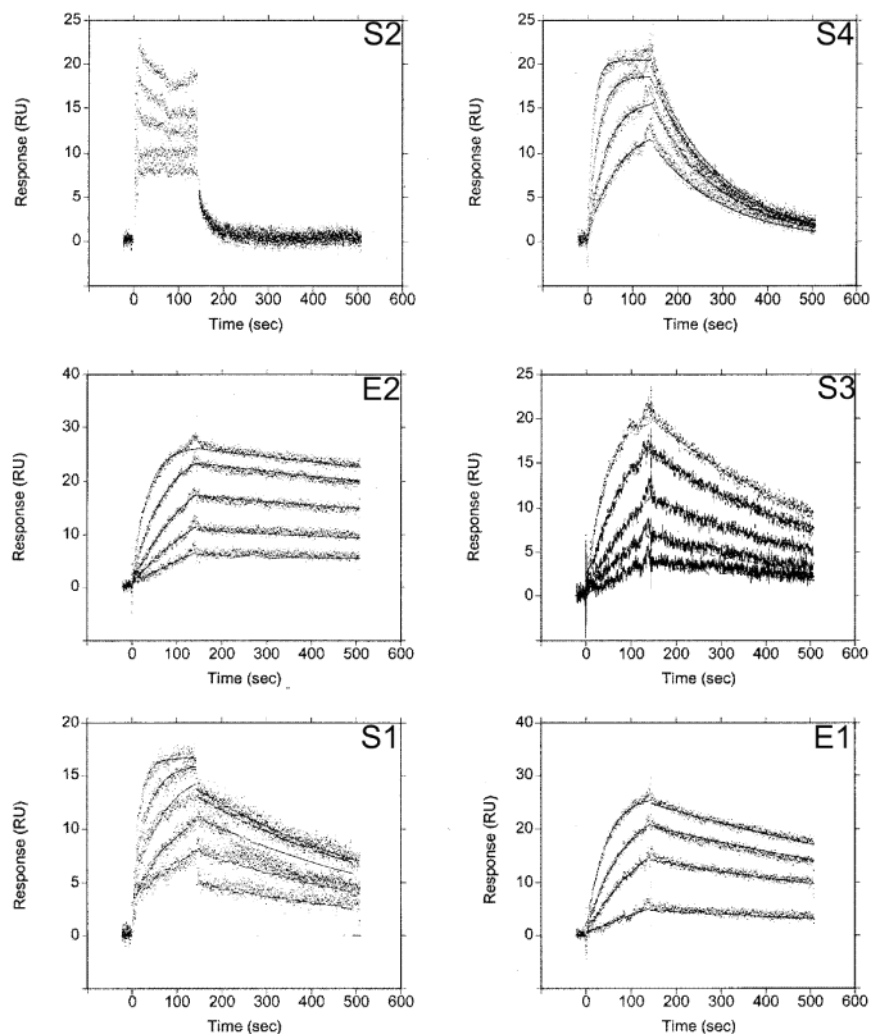
FIGURE 2: Binding kinetics of hMT-SP1-P and each scFv. The name of each scFVv is denoted in the top right corner of each graph. The hMT-SP1-P (50 RU) was immobilized onto a CM5 chip. Each scFv was injected onto the CM5 chip at 50 μL min^{-1}. Sensograms of surface plasmon resonance were obtained with concentrations of each scFv ranging from $0.2K_d$ to $5K_d$ of each scFv. The use of very low MT-SP1 density on the chip (50 RU) minimized the mass transfer and rebinding problems affecting the k_{on} value. Single injections of S4 (2 nM) at 5, 15, 50, 75, and 100 μL min^{-1} showed mass transfer-associated deviations at 5 μL min^{-1}, but the sensograms for 15, 50, 75, and 100 were essentially identical. Determination of kinetic parameters for S4 was performed at 50 and 100 μL min^{-1} flow rates on the same chip. We obtained similar values with a small deviation that reflects a slight difference in protein concentrations between the experiments.
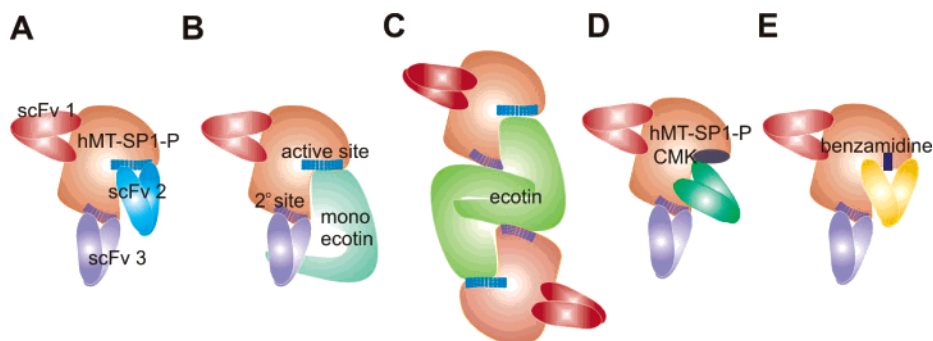

FIGURE 3: Mapping scFvs using ecotin variants. (A) ScFvs 1 (S2) binds to neither the active site nor the secondary site of hMT-SP1-P. ScFv 2 (E1, E2, S1, S3, and/or S4) binds to the active site and scFv 3 binds to the secondary site. The scFvs that bind to the enzyme can be ELISA-positive. (B) The primary site is blocked by mono ecotin, excluding scFv 2. (C) Ecotin competes off both the blue and scFvs 2 and 3. (D) CMK occupies a small area covering the active site. (E) Benzamidine only interacts with the S1 pocket in the active site.

outstanding selectivity, they have great potential to be efficient inhibitors against virtually any biocatalyst. Although inhibitory antibodies targeting proteases have been reported to date, antibodies exhibiting potency and selectivity have not been described (*37−40*). Developing selective and potent inhibitors for proteases is difficult because a target protease

is frequently coexpressed with other similar proteases that differ only slightly in sequence and specificity. One example is the membrane-type serine protease family that currently includes seven human members and the number is still increasing (*4*). The antibody scaffold is an attractive choice for the development of highly potent and selective inhibitors
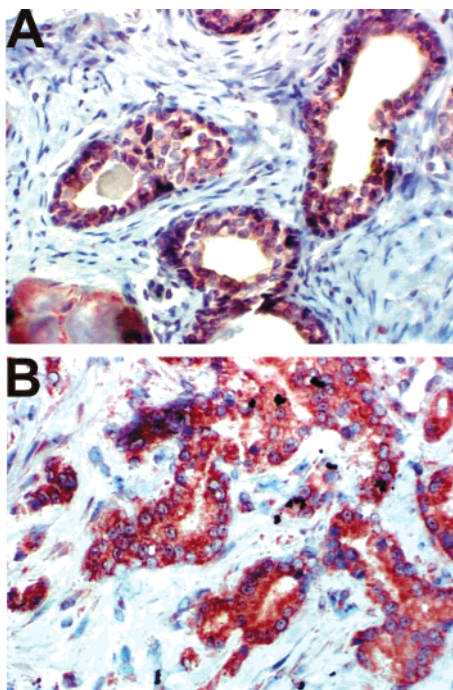
FIGURE 4: Immunostaining (red) of tissues with the S1 detected MT-SP1 in the lumenal membrane from a normal prostate (A) and in the lumenal membrane as well as inside of the lumen in a prostate cancer (B).

for this family since it can immunologically distinguish between closely related proteins. Furthermore, antibodies can easily provide diagnostic and therapeutic reagents. If successful, the method itself can be applied to other enzyme families such as matrix metalloprotease families and protein kinase families.

Regulation of cell surface enzyme activity provides promising specific targets for antibody-based inhibitors. We applied an antibody phage display method to obtain potent and selective antibody protease inhibitors against MT-SP1, a cell surface protease that has emerged as a potential key factor in triggering a proteolytic cascade involved in cancer metastasis. A naïve, synthetic, human antibody library (*21*) was used as a source of single-chain antibodies to screen against hMT-SP1-P.

Since nonspecific binding and low initial concentrations of desired species could easily result in isolating undesired scFv species, an affinity washing procedure was developed. Ecotin was added to the washing solutions to raise stringency in preventing reassociation of released phage by binding to open sites on hMT-SP1-P and the plate. The ecotin used in this affinity washing procedure was an engineered dimeric variant that has a K_i^* of 50 pM for MT-SP1. Although it is a slight difference, ecotin-washing reduced the number of scFvs surviving after each round of panning as well as the number of ELISA-positive variants. Interestingly, the E1 and E2 that were derived from the ecotin-washing pool dissociated slower than other scFvs and E2 was the most potent variant in inhibition as well as in binding (Tables 2 and 3). This implies that the selection pressure of the affinity washing conditions may be the dissociation rate (k_{off}) allowing for selection of scFvs with slow off-rates. Adding a competitive inhibitor in the wash solutions may not interfere with the tightly bound scFvs that dissociate slowly. The use of ecotin in one step of the panning procedure to

result in a more potent inhibitor suggests other possibilities. For example, a similar application in the phage binding or elution steps could result in inhibitors with different modes of binding with increased potency and selectivity.

Inhibition analysis (Table 2) showed that both potency and selectivity was very high in the selected scFvs. The level of potency was up to 50 pM (E2), and the level of selectivity was maximized up to 1500-fold (S4). In the scFv library, the randomized regions are CDR3s of V_H and V_L due to higher solvent exposure. Thus, the variations on these two loop regions, in particular of V_H, enabled these scFvs to clearly discriminate the slight sequence difference between the human and mouse MT-SP1s.

A competition ELISA was devised employing ecotin and mono ecotin to map epitopes on MT-SP1 (Figure 3, Table 4). To narrow down the possible binding modes of these scFvs, the competition ELISA was also performed in the presence of a peptidyl chloromethyl ketone derivative or benzamidine. The ecotin inhibits hMT-SP1-P at 50 pM K_i^* with two binding sites: the active site and a secondary site remote from the active site (*29*) while mono ecotin binds only to the active site with a K_i^* value of 75 nM. The scFvs that are positive in both the ELISAs with the ecotin and the mono ecotin do not bind to either the active site or the secondary site of the protease unless these scFv bind more tightly than the ecotins. These scFvs could be useful allosteric inhibitors of MT-SP1. The scFvs that are positive in the ELISA with mono ecotin and not with ecotin may bind to the protease secondary site or compete more effectively with the mono ecotin for the binding site. This competition ELISA method allowed rapid determination of the binding mode of the scFvs and prioritized our future applications of their binding and inhibitory properties.

A combination of the inhibition assays, binding kinetic analysis, and the competition ELISA provides a more comprehensive description of the binding modes of the scFvs. E1 may not interact with the P1 site because it was positive in the competition ELISA in the presence of benzamidine. S1 competes with monomeric ecotin, but its K_i^* value is 100 fold higher than its K_d value. This suggests that the epitope recognized by S1 may be a different site which is near the active site and not the same site recognized by E2 or S4. Alternatively, since S1 is a strong binder ($K_d = 1.3$ nM) and immunostains fixed tissue slides while other scFvs did not, S1 could recognize a linear epitope still present in MT-SP1 denatured by the fixing process. In contrast, other scFvs might require three-dimensional epitopes. The S3 scFv has a 27-fold higher K_i^* than the K_d. This, in conjunction with the ELISA results, suggests that S3 is likely to act like S1. However, S3 is not effective in immunostaining. Thus, the binding site of the S3 is not the same as the rest of the scFvs. Since the mono ecotin covers a broad area spanning 1900 Å^2, it is also possible that S3 may bind to a site near to but not exactly the active site (*41*).

One reason so many tight-binding antibodies appeared to target the active site may be because it is located in a protein cleft, which has intrinsic physicochemical properties that are favorable to protein−protein interactions (*42*). In this cleft, there are several Ω-loops that are positioned on the surface of the protein so as to be exposed and serve as epitopes for the possible binding in several different modes (*43, 44*). Recently, the catalytic domain of human MT-SP1 was

crystallized in complexes with benzamidine and basic pancreatic trypsin inhibitor (BPTI), and the structures were solved to 1.3 and 2.9 Å, respectively (*45*). These structures illustrate that hMT-SP1-P has a unique 60s-loop in the active site that is nine amino acids longer than in other trypsin-fold serine proteases, which may strongly influence the interaction between the enzyme and scFvs.

As indicated in Tables 2 and 3, S2 inhibits and binds to the antigen with far lower affinity than the other scFvs. ELISA experiments (Figure 3, Table 4) showed that it binds to neither the active site nor the secondary site of hMT-SP1-P. Because S2 did not have to compete for binding to the antigen with the ecotins, this scFv may have survived the affinity-based washing conditions. However, the weakness of the binding affinity of this scFv suggests another possible selection mode. This scFv may have been selected against a denatured epitope to which S2 bound with high affinity during panning or immunoblotting, yet lost its affinity on interacting with native hMT-SP1-P in enzyme activity assays or binding kinetic analyses. Although less likely, several other reasons are possible. S2 could be highly represented in the initial library or expressed at high levels on phage. It may be displayed polyvalently on phage thus allowing an avidity contribution to selection. Alternatively, the amine coupling used for the Biacore experiments may inactivate the S2 binding site giving rise to an apparent weak affinity.

Examination of human tissue sections by IHC showed that the scFv S1 stained human prostate tissues. MT-SP1 is present in normal prostate tissue (Figure 4a) as well as prostate cancer tissue (Figure 4b). However, in addition to being present at the membrane surface of the lumen, it also appeared in the lumenal space of the prostate tumor section suggesting a shedding event. The form of MT-SP1 that is released from the membrane surface may prove to be a useful diagnostic marker for prostate cancer.

In comparison to efforts to develop small molecule inhibitors, in vitro selection of scFvs provides a rapid, general, and robust means to produce potent and selective inhibitors for proteases that are very similar to one another. Furthermore, these scFvs can be used as diagnostic or prognostic reagents. Finally, the therapeutic role of selective protease inhibition can be evaluated in appropriate cancer models by studying the effects of MT-SP1 inhibition on cancer development in vivo. Should the scFvs be sub-optimal to develop as therapeutic agents, an atomic-level understanding of the binding modes of these molecules with their cognate protease may reveal principles that will guide the rational design of small-molecule inhibitors.

ACKNOWLEDGMENT

REFERENCES

1. Andreasen, P. A., Kjoller, L., Christensen, L., and Duffy, M. J. (1997) *Int. J. Cancer 72*, 1−22.
2. Tanimoto, H., Underwood, L. J., Shigemasa, K., Parmley, T. H., Wang, Y., Yan, Y., Clarke, J., and O'Brien, T. J. (1999) *Tumour Biol. 20*, 88−98.
3. Tanimoto, H., Underwood, L. J., Wang, Y., Shigemasa, K., Parmley, T. H., and O'Brien, T. J. (2001) *Tumour Biol. 22*, 104−114.
4. Hooper, J. D., Clements, J. A., Quigley, J. P., and Antails, T. M. (2001) *J. Biol. Chem. 276*, 857−860.
5. Tanimoto, H., Underwood, L. J., Shigemasa, K., Yan, M. S., Clarke, J., Parmley, T. H., and O'Brien, T. J. (1999) *Cancer 86*, 2074−2082.
6. Wallrapp, C., Hahnel, S., Muller-Pillasch, F., Burghardt, B., Iwamura, T., Ruthenburger, M., Lerch, M. M., Adler, G., and Gress, T. M. (2000) *Cancer Res. 60*, 2602−2606.
7. Koblinski, J. E., Ahram, M., and Sloane, B. F. (2000) *Clin. Chim. Acta 291*, 113−135.
8. Hanahan, D., and Weinberg, R. A. (2000) *Cell 100*, 57−70.
9. Sternlicht, M. D., and Werb, Z. (2001) *Annu. Rev. Cell. Dev. Biol. 17*, 463−516.
10. DeClerck, Y. A., Yean, T. D., Lu, H. S., Ting, J., and Langley, K. E. (1991) *J. Biol. Chem. 266*, 3893−3899.
11. Harris, J. L., and Craik, C. S. (2000) *Cell 101*, 136−137.
12. Takeuchi, T., Shuman, M. A., and Craik, C. S. (1999) *Proc. Natl. Acad. Sci. U.S.A. 96*, 11054−11061.
13. Takeuchi, T., Harris, J. L., Huang, W., Yan, K. W., Coughlin, S. R., and Craik, C. S. (2000) *J. Biol. Chem. 275*, 26333−26342.
14. Lin, C. Y., Anders, J., Johnson, M., and Dickson, R. B. (1999) *J. Biol. Chem. 274*, 18237−18242.
15. Lin, C. Y., Anders, J., Johnson, M., Sang, Q. A., and Dickson, R. B. (1999) *J. Biol. Chem. 274*, 18231−18236.
16. Riethmuller, G., Schneider-Gadicke, E., and Johnson, J. P. (1993) *Curr. Opin. Immunol. 5*, 732−739.
17. Huston, J. S., Mudgett-Hunter, M., Tai, M. S., McCartney, J., Warren, F., Haber, E., and Oppermann, H. (1991) *Methods Enzymol. 203*, 46−88.
18. Huston, J. S., Levinson, D., Mudgett-Hunter, M., Tai, M. S., Novotny, J., Margolies, M. N., Ridge, R. J., Bruccoleri, R. E., Haber, E., and Crea, R. (1988) *Proc. Natl. Acad. Sci. U.S.A. 85*, 5879−5883.
19. Hoogenboom, H. R., and Winter, G. (1992) *J. Mol. Biol. 227*, 381−388.
20. Marks, J. D., Hoogenboom, H. R., Griffiths, A. D., and Winter, G. (1992) *J. Biol. Chem. 267*, 16007−16010.
21. Knappik, A., Ge, L., Honegger, A., Pack, P., Fischer, M., Wellnhofer, G., Hoess, A., Wolle, J., Plückthun, A., and Virnekas, B. (2000) *J. Mol. Biol. 296*, 57−86.
22. Winter, G. (1998) *FEBS Lett. 430*, 92−94.
23. Soderlind, E., Strandberg, L., Jirholt, P., Kobayashi, N., Alexeiva, V., Aberg, A. M., Nilsson, A., Jansson, B., Ohlin, M., Wingren, C., Danielsson, L., Carlsson, R., and Borrebaeck, C. A. (2000) *Nat. Biotechnol. 18*, 852−856.
24. Jirholt, P., Ohlin, M., Borrebaeck, C. A., and Soderlind, E. (1998) *Gene 215*, 471−476.
25. Krebber, A., Bornhauser, S., Burmester, J., Honegger, A., Willuda, J., Bosshard, H. R., and Plückthun, A. (1997) *J Immunol. Methods 201*, 35−55.
26. Kaighn, M. E., Narayan, K. S., Ohnuki, Y., Lechner, J. F., and Jones, L. W. (1979) *Invest. Urol. 17*, 16−23.
27. Williams, J. W., and Morrison, J. F. (1979) *Methods Enzymol. 63*, 437−467.
28. Yang, S. Q., and Craik, C. S. (1998) *J. Mol. Biol. 279*, 1001−1011.
29. Yang, S. Q., Wang, C. I., Gillmor, S. A., Fletterick, R. J., and Craik, C. S. (1998) *J. Mol. Biol. 279*, 945−957.
30. Eggers, C. T., Wang, S. X., Fletterick, R. J., and Craik, C. S. (2001) *J. Mol. Biol. 308*, 975−991.
31. Gillmor, S. A., Takeuchi, T., Yang, S. Q., Craik, C. S., and Fletterick, R. J. (2000) *J. Mol. Biol. 299*, 993−1003.
32. Mundorff, E. C., Hanson, M. A., Varvak, A., Ulrich, H., Schultz, P. G., and Stevens, R. C. (2000) *Biochemistry 39*, 627−632.
33. Schultz, P. G. (1998) *Proc. Natl. Acad. Sci. U.S.A. 95*, 14590−14591.
34. Yu, J., Choi, S. Y., Moon, K. D., Chung, H. H., Youn, H. J., Jeong, S., Park, H., and Schultz, P. G. (1998) *Proc. Natl. Acad. Sci. U.S.A. 95*, 2880−2884.
35. Ulrich, H. D., Mundorff, E., Santarsiero, B. D., Driggers, E. M., Stevens, R. C., and Schultz, P. G. (1997) *Nature 389*, 271−275.
36. Wedemayer, G. J., Patten, P. A., Wang, L. H., Schultz, P. G., and Stevens, R. C. (1997) *Science 276*, 1665−1669.

37. Yi, J., Cheng, H., Andrake, M. D., Dunbrack, R. L., Roder, H., and Skalka, A. M. (2002) *J. Biol. Chem. 277*, 12164−12174.

38. Tsuda, T., Ohmori, Y., Muramatsu, H., Hosaka, Y., Takiguchi, K., Saitoh, F., Kato, K., Nakayama, K., Nakamura, N., Nagata, S., and Mochizuki, H. (2001) *Eur. J. Pharmacol. 433*, 37−45.

39. Martin, F., Steinkühler, C., Brunetti, M., Pessi, A., Cortese, R., Francesco, R., and Sollazzo, M. (1999) *Protein Eng. 12*, 1005−1011.

40. Dickinson, C. D., Shobe, J., and Ruf, W. (1998) *J. Mol. Biol. 277*, 959−971.

41. McGrath, M. E., Erpel, T., Bystroff, C., and Fletterick, R. J. (1994) *EMBO J. 13*, 1502−1507.

42. DeLano, W. L., Ultsch, M. H., de Vos, A. M., and Wells, J. A. (2000) *Science 287*, 1279−1283.

43. Driscoll, J. E., Seachord, C. L., Lupisella, J. A., Darveau, R. P., and Reczek, P. R. (1996) *J. Biol. Chem. 271*, 22969−22975.

44. Kanyo, Z. F., Pan, K. M., Williamson, R. A., Burton, D. R., Prusiner, S. B., Fletterick, R. J., and Cohen, F. E. (1999) *J. Mol. Biol. 293*, 855−863.

45. Friedrich, R., Fuentes-Prior, P., Ong, E., Coombs, G., Hunter, M., Oehler, R., Pierson, D., Gonzalez, R., Huber, R., Bode, W., and Madison, E. L. (2002) *J. Biol. Chem. 277*, 2160−2168.